

Nucleophilic Aromatic Substitution of 2-(3(5)-Pyrazolyl)pyridine: A Novel Access to Multidentate Chelate Ligands

Katrin Rößler^a, Tobias Kluge^a, Anett Schubert^a, Yu Sun^{a,b}, Eberhardt Herdtweck^c, and Werner R. Thiel^{a,b}

^a Institut für Chemie, Technische Universität Chemnitz, Straße der Nationen 62, D-09111 Chemnitz, Germany

^b *New address:* Fachbereich Chemie, Technische Universität Kaiserslautern, Erwin-Schrödinger-Str. Geb. 54, D-67663 Kaiserslautern, Germany

^c Anorganisch-chemisches Institut, Technische Universität München, Lichtenbergstr. 4, D-85748 Garching, Germany

Reprint requests to Prof. Dr. W. R. Thiel. thiel@chemie.uni-kl.de

Z. Naturforsch. **59b**, 1253 – 1263 (2004); received August 5, 2004

Dedicated to Professor Hubert Schmidbaur on the occasion of his 70th birthday

1-(Nitrophenyl) functionalized 2-(3-pyrazolyl)pyridines were obtained by a nucleophilic aromatic substitution and could be reduced to the corresponding aminophenyl substituted derivatives. These compounds can be used to co-ordinate transition metal sites or for the generation of building blocks for supramolecular chemistry. The solid state structure of a 1,1'-functionalized ferrocene, which was obtained following this route, is discussed in detail.

Key words: Chelate Ligands, Ferrocene, Nucleophilic Aromatic Substitution

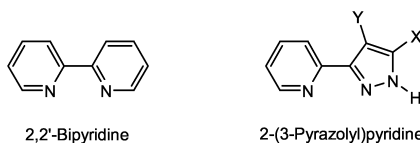
Introduction

Moderate changes in the structure of a well known ligand system may strongly and predictably influence its co-ordination behavior and thus the chemical and physical properties of related metal complexes. This is one of the main impulsions keeping research in “ligand design” running and has led to tremendous progress in economically important fields like catalysis or material science. But ligand design may also make chemists’ life easier.

2,2'-Bipyridine, for example, one of the mostly used *N,N*-chelate ligands and its metal complexes have been under investigation for long. However, there are just a few alkylated derivatives commercially available but no 2,2'-bipyridines bearing “real” functionalities. This is due to the facts that the pyridine rings are deactivated heteroaromatics that don't undergo substitution reactions and that the total synthesis of 2,2'-bipyridines is still not generalized for a broad series of substituents. Therefore detailed investigations in structure / activity relations of substituted 2,2'-bipyridine complexes are rare.

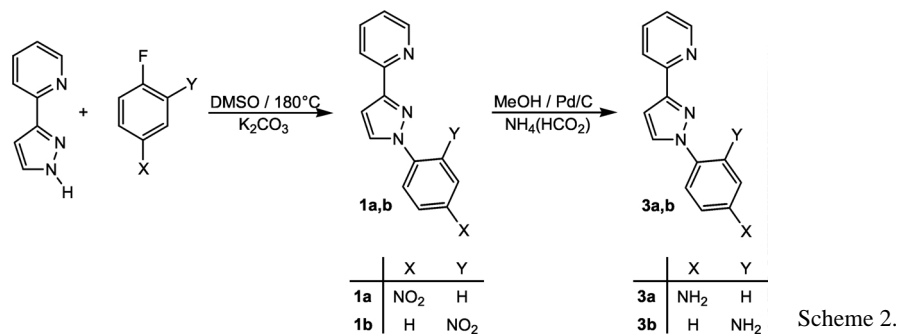
To overcome this problem, we have been working on 2-(3(5)-pyrazolyl)pyridines for some time. This

N,N-chelate ligand [1], which was not frequently used in coordination chemistry, is structurally and electronically closely related to 2,2'-bipyridine (Scheme 1, only the 2-(3-pyrazolyl)pyridine tautomer is shown). However, the pyrazole site can be synthesized from different substituted and commercially available precursors and can additionally be functionalized in the 4-position by electrophilic aromatic substitution [2]. Since the N-H group allows further reactions at the N1 nitrogen atom, a whole panoply of tailor-made chelating systems is accessible [2a, 3].



Scheme 1.

Derivatives of 2-(3-pyrazolyl)pyridine bearing an *N*-phenyl motif instead of the N-H group can be synthesized by ring closure of a 3-(2-pyridyl)propan-1,3-dion with *N*-phenyl hydrazine. However, this will lead to a mixture of regio isomers and thus will cause additional efforts for the purification of the ligand. Since 1-alkylated members of this ligand family can



be obtained by a deprotonation (with NaH) / nucleophilic aliphatic substitution (with RX) sequence in high yields, an analogous procedure for the implementation of aromatic substituents in the 1-position should be developed. This will open up an access to novel functionalized multidentate ligands with potential applications in catalysis and supramolecular chemistry.

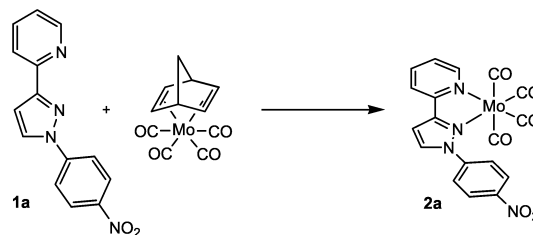
Results and Discussion

For undergoing nucleophilic aromatic substitution, a certain substitution pattern is required at the benzene substrate, including at least one strongly electron withdrawing group. We chose 2- and 4-nitrofluoro benzene as starting material, since the fluoride has turned out to be an excellent leaving group for this reaction and the nitro function can easily be reduced to an NH₂-group, which will allow doing chemistry at that site. Pyrazoles and related compounds have frequently been used as nucleophiles for aromatic substitution reactions [4]. However, 2-(3(5)-pyrazolyl)pyridines have only been reported in combination with 2-bromopyridine and ethyl 4-fluorobenzoate as substrates [5].

Reacting 2- and 4-nitrofluoro benzene with 2-(3(5)-pyrazolyl)pyridine in DMSO solution in the presence of K₂CO₃ as the base, gives the corresponding 1-nitrophenyl functionalized 2-(3-pyrazolyl)pyridines **1a** and **1b** in excellent yields as yellow colored solids (Scheme 2). The formation of the isomers with the nitrophenyl group in the 2-position at the pyrazole ring is not observed, probably due to steric hindrance of the pyridyl ring.

Reacting the less sterically hindered nitro derivative **1a** with (nor)Mo(CO)₄ (nor = norbornadiene) gives the *N,N'*-chelate complex **2a** in good yields (Scheme 3).

Crystals suitable for X-ray analysis were grown from slow diffusion of diethylether into a concentrated solution of **2a** in CH₂Cl₂ at room temperature. **2a** crys-



Scheme 3.

tallizes as dark red blocks in the monoclinic space group *P*2₁/*c* with four molecules in the unit cell. The molecular structure and characteristic bond parameters are presented in Fig. 1 and the arrangement of the molecules in the unit cell is presented in Fig. 2. Complex **2a** is just the second structurally characterized tetracarbonyl molybdenum complex with a nitrophenyl substituted ligand up to now [6].

All bond lengths and angles of **2a** are comparable to those of analogous tetracarbonyl molybdenum complexes bearing a chelate ligand with two sp² hybridized nitrogen donor sites [9, 10]. The pyridyl and the pyrazolyl ring as well as the phenyl ring and the nitro group are found in an almost coplanar orientation, while the torsion angle between the pyrazolyl and the phenyl ring is about 121°, mainly due to the repulsive interactions between the phenyl ring and one of the carbonyl ligands and especially between H8 and H10/H14.

The IR spectrum of **2a** is dominated by four CO absorptions, which are observed at almost the same wavenumbers as in the only other structurally characterized Mo(CO)₄ complex bearing a pyrazolylpyridine ligand [10]. A strong shift to lower field of the ¹H NMR resonance of the *ortho* pyridine proton H¹¹ is characteristic for a coordination of the chelate ligand [2]. The resonances of the protons H⁸ and H⁴, which are next to the central C-C bond between the pyridine and the pyrazole moiety, are shifted to higher

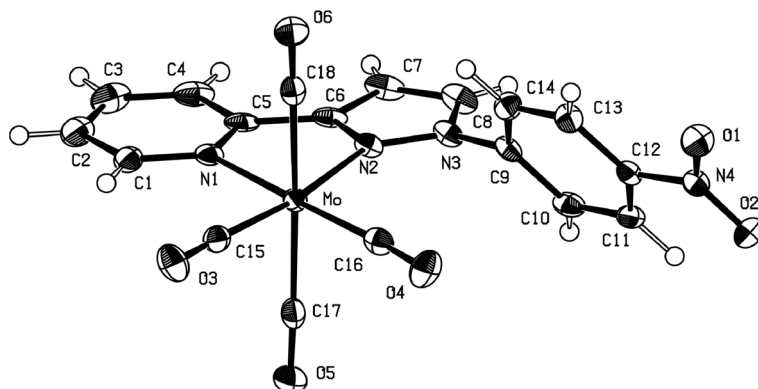


Fig. 1. ORTEP [7] plot of the solid state structure of **2a**. Thermal ellipsoids are drawn at the 50% probability level. Selected bond lengths [Å], angles [°] and torsion angles [°]: Mo–N1 2.2733(18), Mo–N2 2.2487(18), Mo–C15 1.963(2), Mo–C16 1.964(2), Mo–C17 2.040(3), Mo–C18 2.057(3), N1–Mo–N2 71.66(7), N1–Mo–C15 100.06(8), N1–Mo–C16 173.15(8), N1–Mo–C17 91.32(8), N1–Mo–C18 91.87(8), N2–Mo–C15 171.37(8), N2–Mo–C16 102.36(8), N2–Mo–C17 95.40(8), N2–Mo–C18 90.12(8), C15–Mo–C16 86.04(9), C15–Mo–C17 87.06(9), C15–Mo–C18 87.70(9), C16–Mo–C17 85.84(10), C16–Mo–C18 91.50(10), C17–Mo–C18 174.28(8), Mo–C15–O3 177.44(18), Mo–C16–O4 176.6(2), Mo–C17–O5 173.75(18), Mo–C18–O6 177.65(17), N1–C5–C6–N2 0.5(3), N2–N3–C9–C10 121.3(2), O1–N4–C12–C11 175.7(2).

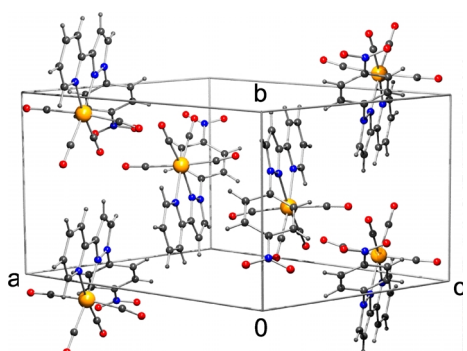
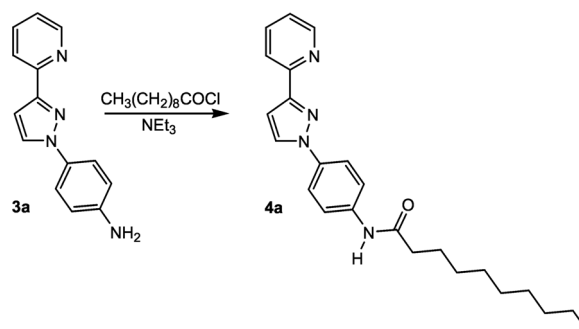


Fig. 2. PLUTON [8] plot of the solid state structure of **2a**.

field, due to an increased shielding by the coplanar chelate system. In the ^{13}C NMR, the three different carbonyl ligands can clearly be distinguished: the resonances of the equatorial CO ligands are observed at 223.5, and 222.1 ppm and the resonances of the axial CO ligands are observed at 205.8 ppm.

Pd/C catalyzed reduction of the nitro group with ammonium formate gives the corresponding amino derivatives **3a** and **3b** as colorless solids in yields of about 80% (Scheme 2). IR spectroscopy proves the complete conversion of the nitro into the amino group by the disappearance of the strong absorptions of the nitro group and new bands in the range of 3450–3200 cm^{-1} which are typical for mono substituted aromatic amines. While the resonances of the protons at the pyridine and the pyrazole ring are almost unaffected by this transformation, the resonances of H^{13}



Scheme 4.

and H^{14} are as expected significantly shifted to higher field.

Since neither from **3a** nor from **3b** crystals suitable for single crystal X-ray structure analysis could be grown, **3a** was substituted with a long alkyl side chain by reacting with decanoic acid chloride (Scheme 4). The resulting decanoic anilide **4a** could be recrystallized from ethyl acetate giving crystals of X-ray quality.

4a crystallizes as colorless blocks in the monoclinic space group $C2/c$ with eight molecules in the unit cell. As expected, the acidic amide proton undergoes hydrogen bonding with the most basic proton acceptor, the pyridine nitrogen atom. This results in the formation of hydrogen bound polymeric chains. The molecular structure and characteristic bond parameters of **4a** are presented in Fig. 3 and the arrangement of the

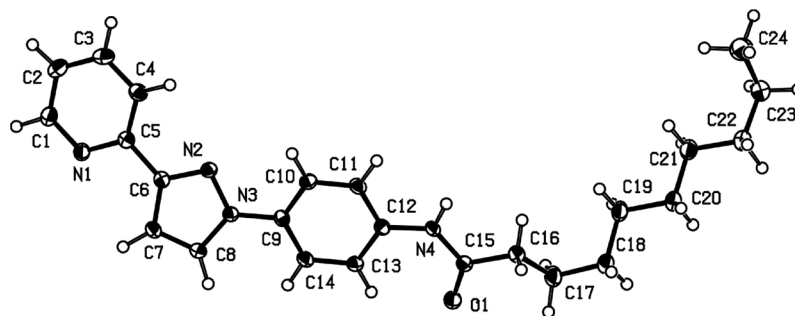


Fig. 3. ORTEP [7] plot of the solid state structure of **4a**. Thermal ellipsoids are drawn at the 50% probability level. Selected bond lengths [Å], angles [°] and torsion angles [°]: N4–C15 1.360(2), O1–C15 1.2247(16), N4–H4 0.882(16), H4...N1' 2.106(17), N4...N1' 2.9858(16), C12–N4–C15 128.68(11), O1–C15–N4 123.95(12), O1–C15–C16 121.83(14), N4–C15–C16 114.21(12), C15–N4–H4 114.9(13), N4–H4...N1' 175.2(18), N1–C5–C6–N2 165.24(12), N2–N3–C9–C14 –157.63(12), C15–N4–C12–C11 –178.14(13), C12–N4–C15–C16 –177.16(13), C16–C17–C18–C19 –72.08(19), C21–C22–C23–C24 70.0(2). The symmetry operation for N' is: $x, -y, -0.5 + z$.

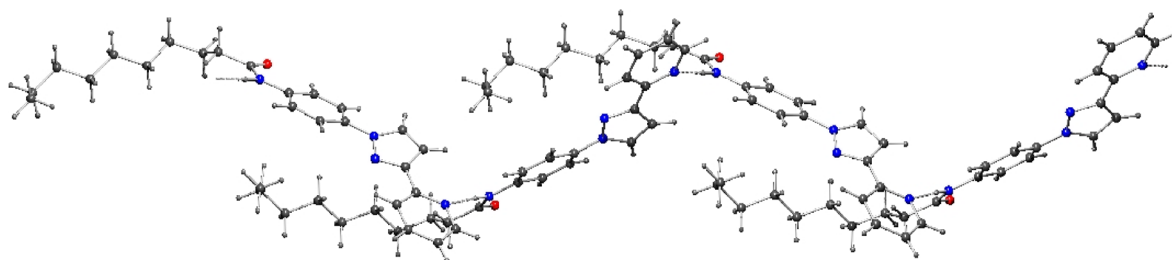


Fig. 4. PLUTON [8] plot of the solid state structure of **4a** showing the hydrogen bond chains running along the c -axis.

polymeric chain by hydrogen bonding is presented in Fig. 4.

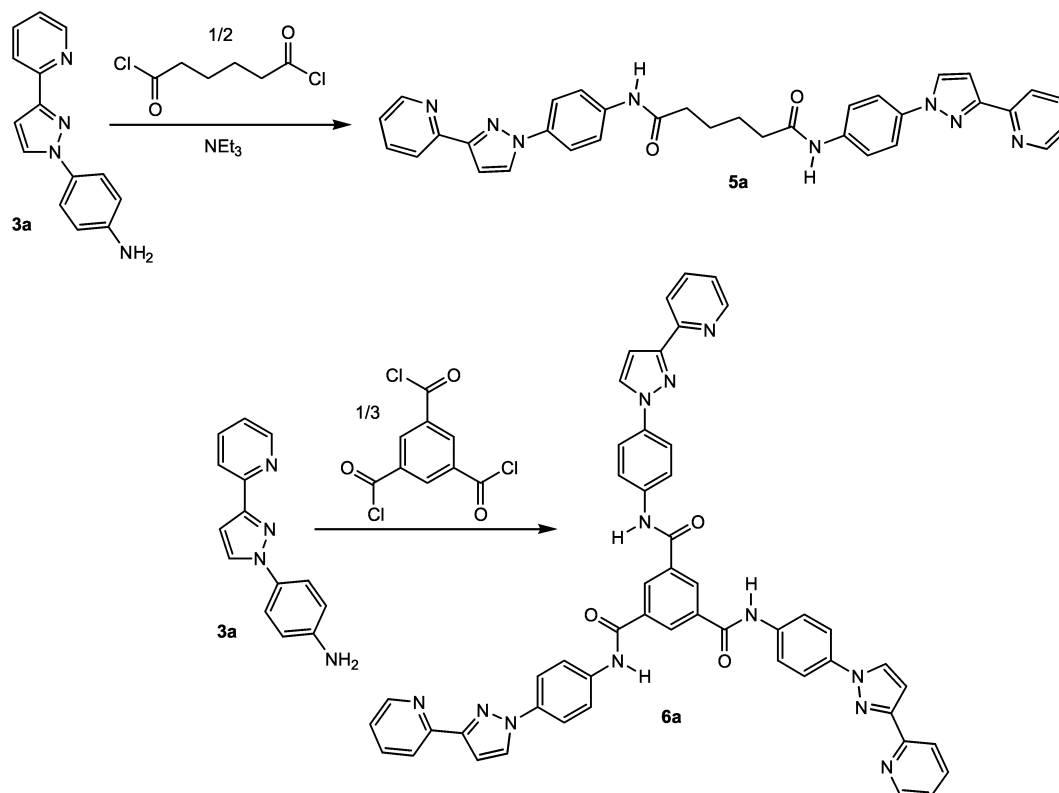
The *all-trans* configuration of the $\text{CH}_3(\text{CH}_2)_8$ chain (torsion angles $\text{C}=\text{C}-\text{C}=\text{C} = 180^\circ$), which would be energetically favored for an isolated molecule, is not completely realized in the solid state structure of **4a**. The torsion angles C16–C17–C18–C19 and C21–C22–C23–C24 are about 70° , probably due to packing effects. This leads, in combination with the torsions of the aromatic part of the molecule, to a banana-like shape of **4a** in the solid state. While the pyridine, the pyrazole, and the phenyl ring are slightly twisted out of coplanarity (N1–C5–C6–N2: 165.2° , N2–N3–C9–C14 -157.6°), the almost planar amide group (C12–N4–C15–C16 -177.2°) is oriented coplanar to the phenyl substituent (C15–N4–C12–C11 -178.1°). The bond parameters for the hydrogen bond forming atoms N4–H4...N1' (N4–H4: 0.882 Å, H4...N1': 2.106 Å, N4...N1': 2.986, N4–H4...N1': 175.2°) are typical for a hydrogen bond of medium strength and are corroborating with the data from structurally characterized hydrogen bonds between pyridines and carboxylic acid amides [11, 12].

The transformation of the amine into the amide is associated with changes in the IR and NMR spectra. In the infrared spectrum of **4a**, the typical N–H stretching mode of an associated amide at 3190 cm^{-1} and the characteristic absorptions of the amide group at 1689 and 1517 cm^{-1} ($\nu(\text{C}=\text{O})$ and $\nu(\text{N}-\text{C}=\text{O})$) are observed. As expected, only the resonances of the phenylene protons H¹³ and H¹⁴, which are close to the amide function, are shifted significantly to lower field compared to the resonances of **3a**.

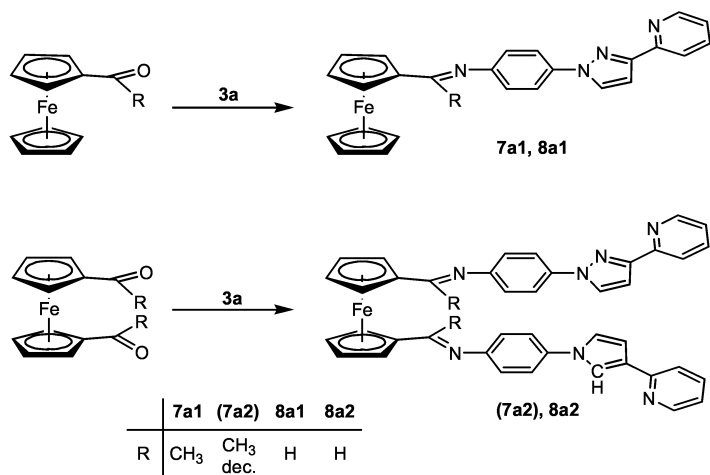
For the generation of building blocks for supramolecular coordination compounds, **3a** was reacted with the divalent adipic acid dichloride and the trivalent benzenetricarboxylic acid trichloride, which yielded the tetra- and hexadentate ligands **5a** and **6a** in almost quantitative yields (Scheme 5).

Due to strong intermolecular hydrogen bonding, the polyanilides **5a** and **6a** are only sparingly soluble in most organic solvents. They are obtained as water adducts. A detailed investigation of the complex chemistry of these multidentate ligands is performed.

The amino groups of **3a** and **3b** additionally open up the possibility to undergo condensation with (acti-



Scheme 5.



Scheme 6.

vated) carbon electrophiles. We chose ferrocenyl containing compounds for these reactions to introduce an organometallic fragment. Due to its electron donating methyl group, acetyl ferrocene only slowly reacts with **3a**. However, the addition of a 1:1 mixture of neutral and acidic alumina accelerates the reaction and enforces the dehydration of the intermediate formed

aminoacetal (Scheme 6). This provides the ferrocenyl substituted imine **7a1** in only 40% yield. Reacting 1,1'-diacetyl ferrocene under the same conditions only results in decomposition, **7a2** could not be obtained.

To prove, whether steric hindrance is responsible for this behavior, we reacted the more electrophilic ferrocenyl mono- and 1,1'-dialdehyde with **3a**. The cor-

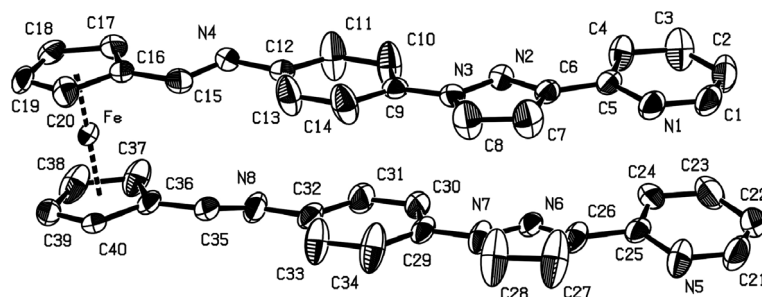


Fig. 5. ORTEP [7] plot of the solid state structure of **8a2**. Thermal ellipsoids are drawn at the 50% probability level. The hydrogen atoms are omitted for clarity. Selected bond lengths [Å], angles [°] and torsion angles [°]: Fe–C16 2.030(3), Fe–C17 2.037(3), Fe–C18 2.044(3), Fe–C19 2.047(3), Fe–C20 2.035(3), Fe–C36 2.052(3), Fe–C37 2.041(3), Fe–C38 2.037(3), Fe–C39 2.041(3), Fe–C40 2.036(3), N4–C15 1.271(3), N8–C35 1.258(4), C12–N4–C15 120.0(2), N4–C15–C16 121.2(3), C32–N8–C35 119.9(2), N8–C35–C36 121.8(3), N1–C5–C6–N2 –172.0(2), N2–N3–C9–C10 2.6(4), C15–N4–C12–C13 –12.1(4), C12–N4–C15–C16 –178.0(3), N4–C15–C16–C17 10.4(5), N5–C25–C26–C27 15.1(5), N6–N7–C29–C30 –5.4(4), C35–N8–C32–C33 19.7(4), C32–N8–C35–C36 –177.9(2), N8–C35–C36–C37 –20.4(5).

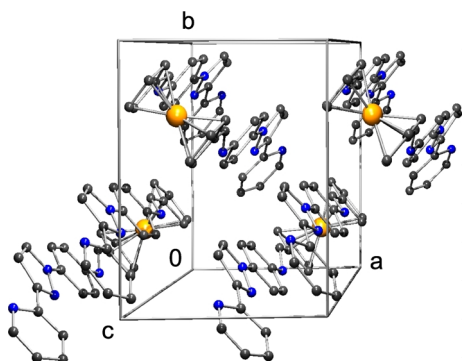


Fig. 6. PLUTON [8] plot of the solid state structure of **8a2** in the unit cell.

responding imines **8a1** and **8a2** could be obtained in good yields without the application of a catalyst. This gives a strong hint, that the intrinsic reactivity of the carbonyl group at the ferrocene moiety is responsible for the success or failure of the condensation.

Crystals suitable for X-ray analysis could be obtained by crystallization of **8a2** from CHCl_3 . The compound crystallizes as deep red blocks in the monoclinic space group $P2_1$ with two molecules in the unit cell. The molecular structure and characteristic bond parameters are presented in Fig. 5 and the arrangement of the molecules in the unit cell is presented in Fig. 6.

Probably due to favourable π - π interactions, the two heteroaromatic side chains are oriented eclipsed (torsion C15–C16–C36–C35: -1.9°) and almost parallel to each other. However, since there is no symmetry element located in the molecule, they show slightly different geometries, which is quite obvious regarding the twists between the ring systems and the torsions of the

imine units. The iron center is located almost below and above the centroids of the Cp rings and the C=N distances are typical for imine units. The bond distances of the core of **8a2** are almost identical with the values of $(\eta^5\text{-C}_5\text{H}_4\text{-CH=N-Ph})_2\text{Fe}$ [13]. However, in the latter compound, the phenyl rings are strongly bent with respect to each other, which allows intramolecular H- π interaction instead of π - π interaction as observed for **8a2**.

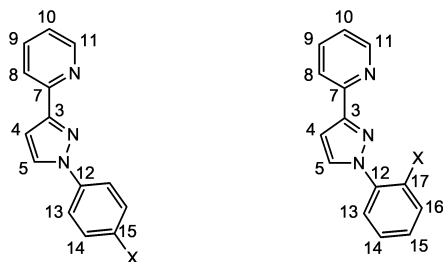
The π - π interactions seem not to play a prominent role in solution (chloroform), since the chemical shifts of the side chains of **8a1** and **8a2** are almost identical, which corroborates with free rotation in solution. As expected, the C=N stretching frequency is shifted about 40 cm^{-1} to lower wave numbers, when the methyl group at the imine function (**7a1**) is replaced by a proton (**8a1** and **8a2**) indicating a stronger C=N bond in **7a1** due to the electron push of the methyl group.

Conclusion

We could show that nucleophilic aromatic substitution of pyrazolyl pyridine (or pyrazoles in general) is a suitable way for the generation of ligands bearing functionalities which are interesting for applications in different fields of inorganic / organometallic chemistry. The compounds presented in this paper are just exemplary, further investigations in this field are in progress.

Experimental Section

General remarks: The syntheses of the all compounds were performed under an atmosphere of argon, solvents were



Scheme 7.

dried and distilled before use. The NMR data are assigned by means of 2D NMR spectroscopy according to the numbering given in Scheme 7.

2-[1-(4-Nitrophenyl)-1H-pyrazol-3-yl]pyridine (1a) and 2-[1-(2-nitrophenyl)-1H-pyrazol-3-yl]pyridine (1b): A solution of 14.50 g (0.10 mol) of 2-(3(5)-pyrazolyl)pyridine and 21.15 g (0.15 mol) of the appropriate fluoronitro benzene in 100 ml of DMSO is treated with 41.46 g (0.30 mol) of anhydrous K_2CO_3 . The mixture is stirred vigorously, heated to 180 °C for 4 h and poured onto crushed ice. The resulting solid is filtered washed with diethylether to remove the excess of fluoronitro benzene, dried in the air and further purified by recrystallization from ethyl acetate. **1a:** 20.84 g (77%) of a yellow microcrystalline solid. IR (KBr): $\nu = 3126w\text{ cm}^{-1}$, 1593s, 1535m, 1518s $\nu(NO_2)_{\text{asym}}$, 1483m, 1455m, 1393m, 1366m, 1333vs $\nu(NO_2)_{\text{sym}}$, 1313s, 1276s, 1112m, 1049m, 1038m, 957w, 939m, 852s, 767m, 749m. 1H NMR (250.13 MHz, 25 °C, DMSO- d_6): $\delta = 8.67$ (d, $^3J_{10,11} = 4.8$ Hz, H^{11}), 8.35 (d, $^3J_{13,14} = 9.1$ Hz, 2H, H^{14}), 8.12 (d, $^3J_{8,9} = 8.0$ Hz, H^8), 8.09 (d, $^3J_{4,5} = 2.6$ Hz, H^5), 7.98 (d, 2H, H^{13}), 7.78 (dt, $^3J_{9,10} = 8.0$ Hz, $^4J_{9,11} = 1.5$ Hz, H^9), 7.29 (dd, H^{10}), 7.21 (d, H^4). $^{13}C\{^1H\}$ NMR (62.895 MHz, 25 °C, DMSO- d_6): $\delta = 154.3$ (C^3), 150.7 (C^7), 149.7 (C^{11}), 145.1, 144.1 (C^{12} , C^{15}), 137.3 (C^9), 130.8 (C^5), 125.6 (C^{13}), 123.8 (C^{10}), 120.2 (C^8), 118.8 (C^{14}), 108.1 (C^4). MS (EI, 70 eV): m/z (%) = 266 (55) $[M]^+$, 220 (8) $[M-NO_2]^+$, 219 (14) $[M-HNO_2]^+$, 117 (12) $[C_8H_7N]^+$, 116 (30) $[C_8H_6N]^+$, 78 (100) $[C_5H_4N]^+$. $C_{14}H_{10}N_4O_2 \cdot (H_2O)_{0.25}$ (270.76): calcd. C 62.10, H 3.91, N 20.69; found C 62.29, H 3.76, N 20.60. **1b:** 26.44 g (98%) of a yellow microcrystalline solid. IR (KBr): $\nu = 3160m\text{ cm}^{-1}$, 3043m, 1607m, 1590m, 1534vs $\nu(NO_2)_{\text{asym}}$, 1501s, 1482m, 1456m, 1421m, 1390m, 1365vs $\nu(NO_2)_{\text{sym}}$, 1303m, 1277m, 1260m, 1048m, 992m, 959m, 946m, 850m, 783m, 764s, 745m, 723m, 701m, 629m. 1H NMR (250.13 MHz, 25 °C, DMSO- d_6): $\delta = 8.67$ (ddd, $^3J_{10,11} = 4.8$ Hz, $^4J_{9,11} = ^5J_{8,11} = 1.3$ Hz, H^{11}), 8.45 (d, $^3J_{4,5} = 2.5$ Hz, H^5), 8.09 (dd, $^3J_{8,9} = 8.0$ Hz, H^8), 7.98–7.84 (m, 3H, H^{13} , H^{15} , H^{16}), 7.70 (dt, $^3J_{9,10} = 8.0$ Hz, H^9), 7.39 (dd, H^{10}), 7.18 (d, H^4). $^{13}C\{^1H\}$ NMR (62.895 MHz, 25 °C, DMSO- d_6): $\delta = 154.3$ (C^3), 151.4 (C^7), 150.1 (C^{11}), 144.5 (C^{17}), 137.7 (C^9), 134.1, 133.1 (C^{12} , C^{14}), 132.7 (C^5), 129.5, 126.1, 125.7 (C^{13} , C^{15} , C^{16}), 123.9 (C^{10}), 120.3

(C^8), 107.2 (C^4). MS (EI, 70 eV): m/z (%) = 266 (31), $[M]^+$, 220 (3) $[M-NO_2]^+$, 130 (49) $[C_9H_6N]^+$, 117 (8) $[C_8H_6N]^+$, 116 (13) $[C_8H_7N]^+$, 105 (21) $[C_7H_7N]^+$, 104 (33) $[C_8H_8]^+$, 92 (14) $[C_6H_6N]^+$, 91 (15) $[C_6H_5N]^+$, 90 (23) $[C_6H_4N]^+$, 89 (35) $[C_6H_3N]^+$, 78 (100) $[C_5H_4N]^+$. $C_{14}H_{10}N_4O_2 \cdot (H_2O)_{0.20}$ (269.86): calcd. C 62.31, H 3.88, N 20.76; found C 62.63, H 3.59, N 20.54.

Tetracarbonyl{2-[1-(4-nitrophenyl)-1H-pyrazol-3-yl]-pyridine}molybdenum(0) (2a): 135 mg (0.50 mmol) of **1a** and 150 mg (0.50 mmol) of (nor)Mo(CO)₄ (nor = norbornadiene) are suspended in 20 ml of toluene. The yellow suspension is heated to 70 °C for 30 min, whereby the color turns to orange-red and the solid dissolves. The solution is filtered through a Whatman® pad and the product is crystallized at –20 °C. The microcrystalline solid is washed with 20 ml of diethylether and dried in the vacuum. Yield: 151 mg (63%) of an orange-red, microcrystalline solid. IR (KBr): $\nu = 3148w\text{ cm}^{-1}$, 3119w, 3083w, 2015s, 1897vs, 1869vs, 1812vs $4 \times \nu$ (CO), 1591m, 1515s $\nu(NO_2)_{\text{asym}}$, 1436m, 1345s $\nu(NO_2)_{\text{sym}}$, 1272m, 1114m, 1054m, 853s, 767s, 607m, 581m, 551m. 1H NMR (250.13 MHz, 25 °C, CDCl₃): $\delta = 9.07$ (d, $^3J_{10,11} = 5.4$ Hz, H^{11}), 8.47 (d, $^3J_{13,14} = 8.7$ Hz, 2H, H^{14}), 7.93 (d, $^3J_{4,5} = 2.7$ Hz, H^5), 8.00 (d, $^3J_{8,9} = 7.4$ Hz, H^8), 7.85 (t, H^9), 7.82 (d, 2H, H^{13}), 7.33 (t, H^{10}), 7.08 (d, H^4). $^{13}C\{^1H\}$ NMR (62.895 MHz, 25 °C, acetone- d_6): $\delta = 223.5$, 222.1 ($2 \times CO_{\text{eq}}$), 205.8 (CO_{ax}), 155.3 (C^3), 154.7 (C^{11}), 152.8 (C^7), 150.0 (C^{12}), 145.5 (C^{15}), 140.2 (C^9), 138.0 (C^5), 128.6 (C^{13}), 126.4 (C^{10}), 126.3 (C^{14}), 124.3 (C^8), 108.3 (C^4). $C_{18}H_{10}MoN_4O_6$ (474.24): calcd. C 45.59, H 2.13, N 11.81; found C 46.12, H 2.35, N 11.75.

2-[1-(4-Aminophenyl)-1H-pyrazol-3-yl]pyridine (3a) and 2-[1-(2-aminophenyl)-1H-pyrazol-3-yl]pyridine (3b): 0.25 g of Pd/C (10% Pd, Aldrich 20,569-9) are added under an atmosphere of nitrogen to a solution of 9.46 g (0.15 mol) of $NH_4(HCO_2)$ dissolved in 100 ml of MeOH. When hydrogen evolution has started, 8.10 g (0.03 mol) of the appropriate nitro compound **1a** or **1b** are added and the mixture is heated to reflux for 2 h. After cooling to room temperature, the solution is filtrated to remove Pd/C, the solvent is removed in vacuum and the colorless solid residue is washed with water to remove $NH_4(HCO_2)$ and $NH_4(HCO_3)$ and dried in the air. **3a:** 5.74 g (81%) of a colorless microcrystalline solid. IR (KBr): $\nu = 3438m\text{ cm}^{-1}$, 3334s, 3214s $3 \times \nu(NH_2)$, 1634s, 1513vs, 1458m, 1422m, 1264m, 1052m, 828s, 771s, 622m. 1H NMR (250.13 MHz, 25 °C, CDCl₃): $\delta = 8.64$ (dd, $^3J_{10,11} = 4.9$ Hz, $^4J_{9,11} = 1.7$ Hz, H^{11}), 8.09 (d, $^3J_{8,9} = 8.0$ Hz, H^8), 7.82 (d, $^3J_{5/4} = 2.4$ Hz, H^5), 7.72 (dt, $^3J_{9,10} = 8.0$ Hz, H^9), 7.52 (d, 2H, $^3J_{13,14} = 8.7$ Hz, H^{13}), 7.21 (ddd, $^4J_{8,10} = 1.5$ Hz, H^{10}), 7.07 (d, H^4), 6.74 (d, 2H, H^{14}), 3.73 (br, NH_2). $^{13}C\{^1H\}$ NMR (62.895 MHz, 25 °C, CDCl₃): $\delta = 152.6$, 152.4 (C^3 , C^7), 149.5 (C^{11}), 145.5 (C^{15}), 136.6 (C^9), 132.4 (C^{12}), 128.4 (C^5), 122.5 (C^{10}), 121.2 (C^{13}), 120.3 (C^8), 115.5

(C¹⁴), 105.8 (C⁴). MS (EI, 70 eV): m/z (%) = 236 (100) [M]⁺, 235 (67) [M-H]⁺, 208 (14) [M-CH₂N]⁺, 131 (23) [C₈H₇N₂]⁺, 118 (15) [C₇H₆N₂]⁺, 105 (19) [C₇H₈N]⁺, 104 (30) [C₇H₇N]⁺, 92 (21) [C₆H₆N]⁺, 78 (71) [C₅H₄N]⁺. C₁₄H₁₂N₄ (236.26): calcd. C 71.16, H 5.12, N 23.71; found C 70.85, H 5.08, N 23.42. **3b**: 5.60 g (79%) of a colorless microcrystalline solid. IR (KBr): ν = 3412s cm⁻¹, 3316m, 3207m 3 × ν (NH₂), 1629s, 1595m, 1566m, 1504vs, 1484m, 1459s, 1424m, 1388m, 1363m, 1291m, 1259m, 1155w, 1050m, 994w, 943w, 764vs, 713m, 669m. ¹H NMR (250.13 MHz, 25 °C, DMSO-d₆): δ = 8.64 (dd, ³J_{10,11} = 4.7 Hz, ⁴J_{9,11} = 1.3 Hz, H¹¹), 8.19 (d, ³J_{4,5} = 2.4 Hz, H⁵), 8.04 (d, ³J_{8,9} = 7.9 Hz, H⁸), 7.86 (dt, ³J_{9,10} = 7.9 Hz, H⁹), 7.34 (ddd, ⁴J_{8,10} = 1.1 Hz, H¹⁰), 7.32 (dd, ³J_{13,14} = 7.9 Hz, ⁴J_{13,15} = 1.4 Hz, H¹³), 7.15 (dt, ³J_{14,15} = ³J_{15,16} = 7.6 Hz, H¹⁵), 7.08 (d, H⁴), 6.94 (dd, ⁴J_{13,15} = 1.1 Hz, H¹⁶), 6.70 (dt, H¹⁴), 5.68 (br, NH₂). ¹³C{¹H} NMR (62.895 MHz, 25 °C, DMSO-d₆): δ = 151.8 (C³), 151.3 (C⁷), 149.3 (C¹¹), 141.8 (C¹⁷), 136.9 (C⁹), 132.3 (C⁵), 128.4 (C¹⁵), 125.2 (C¹²), 124.0 (C¹³), 122.9 (C¹⁰), 119.6 (C⁸), 116.7 (C¹⁶), 116.2 (C¹⁴), 105.0 (C⁴). MS (EI, 70 eV): m/z (%) = 236 (91) [M]⁺, 235 (35) [M-H]⁺, 220 (23) [M-NH₂]⁺, 208 (13) [M-CH₂N]⁺, 158 (15) [C₉H₈N₃]⁺, 132 (50) [C₈H₈N₂]⁺, 131 (75) [C₈H₇N₂]⁺, 119 (31) [C₈H₇N]⁺, 118 (22) [C₈H₆N]⁺, 105 (40) [C₇H₈N]⁺, 104 (37) [C₇H₇N]⁺, 92 (25) [C₆H₆N]⁺, 79 (47) [C₅H₅N]⁺, 78 (100) [C₅H₄N]⁺. C₁₄H₁₂N₄ (236.26): calcd. C 71.16, H 5.12, N 23.71; found C 71.05, H 5.06, N 23.61.

Decanoic acid(4-(3-(2-pyridyl)pyrazol-1-yl)anilide (**4a**), *adipinic acid*(4-(3-(2-pyridyl)pyrazol-1-yl)anilide (**5a**), *benzenetricarboxylic acid*(4-(3-(2-pyridyl)pyrazol-1-yl)anilide (**6a**)): A solution of 10 mmol of the appropriate acid chloride dissolved in 20 ml of CHCl₃ is added dropwise to a solution of an equimolar amount (10 mmol for **4a**, 20 mmol for **5a**, 30 mmol for **6a**) of **3a** and 10 mmol of NEt₃ in 50 ml of toluene. The solution is heated to reflux for 4 h, then the solvent is removed in vacuum and the solid residue is washed thoroughly with water to remove (HNEt₃)Cl. The anilides are obtained in yields of 80–95% as pale yellow colored solids. **4a** was recrystallized from ethyl acetate. **4a**: IR (KBr): ν = 3249w cm⁻¹, 3190w, 3117s, 3045m, 3015m, 2956s, 2921vs, 2854s, 1689vs ν (C=O), 1613m, 1600m, 1554s, 1517vs ν (N–C=O), 1491m, 1459m, 1417m, 1368s, 1331m, 1315m, 1279m, 1252s, 1198w, 1176w, 1062m, 1000w, 945w, 844s, 766s, 736m, 514w. ¹H NMR (250.13 MHz, 25 °C, CDCl₃): δ = 8.63 (dd, ³J_{10,11} = 4.9 Hz, ⁴J_{9,11} = 1.6 Hz, H¹¹), 8.08 (d, ³J_{8,9} = 8.1 Hz, H⁸), 7.91 (br, H⁵), 7.73 (dt, ³J_{9,10} = 7.9 Hz, H⁹), 7.79–7.69 (m, 4H, H¹³, H¹⁴), 7.22 (ddd, ⁴J_{8,10} = 1.1 Hz, H¹⁰), 7.09 (br, H⁴), 2.34 (t, 2H, ³J_{H,H} = 7.6 Hz, C(O)CH₂CH₂), 1.85 (br, NH), 1.60 (q, 2H, C(O)CH₂CH₂), 1.25 (br, 12H, 6 × CH₂), 0.86 (t, 3H, ³J_{H,H} = 6.5 Hz, CH₃). ¹³C{¹H} NMR (62.895 MHz,

25 °C, DMSO-d₆): δ = 171.8 (CO), 152.9 (C³), 152.0 (C⁷), 149.9 (C¹¹), 138.6 (C⁹), 137.2 (C¹⁵), 135.4 (C¹²), 129.4 (C⁵), 123.3 (C¹⁰), 120.2 (C¹³), 120.0 (C⁸), 119.3 (C¹⁴), 106.6 (C⁴), 37.0 (COCH₂CH₂), 31.9 (COCH₂CH₂), 29.5, 29.5, 29.3, 29.3, 25.7 (5 × CH₂), 22.7 (CH₂CH₃), 14.2 (CH₂CH₃). **5a**: IR (KBr): ν = 3116m cm⁻¹, 1671s ν (C=O), 1611m, 1551s, 1517vs ν (N–C=O), 1459m, 1415m, 1368m, 1315m, 1262m, 1176w, 1051w, 946w, 834m, 766m. ¹H NMR (250.13 MHz, 25 °C, DMSO-d₆): δ = 10.16 (s, NH), 8.67 (d, ³J_{10,11} = 4.3 Hz, H¹¹), 8.56 (d, ³J_{4,5} = 2.4 Hz, H⁵), 8.15 (d, ³J_{8,9} = 7.9 Hz, H⁸), 7.97 (t, ³J_{9,10} = 7.9 Hz, H⁹), 7.91, 7.81 (2 × d, 2 × 2H, ³J_{13,14} = 9.2 Hz, H¹³, H¹⁴), 7.44 (dd, H¹⁰), 7.15 (d, H⁴), 3.54 (br, 6H, H₂O), 2.44 (m, COCH₂CH₂), 1.72 (m, COCH₂CH₂). ¹³C{¹H} NMR (62.895 MHz, 25 °C, DMSO-d₆): δ = 171.2 (CO), 151.5 (C³), 150.7 (C⁷), 148.7 (C¹¹), 137.9 (C⁹), 137.8 (C¹⁵), 134.7 (C¹²), 129.4 (C⁵), 123.2 (C¹⁰), 121.1 (C⁸), 120.0 (C¹³), 119.0 (C¹⁴), 106.4 (C⁴), 36.3 (COCH₂CH₂), 24.8 (COCH₂CH₂). C₃₄H₃₀N₈O₂ · (H₂O)₃ (636.71): calcd. C 64.14, H 5.70, N 17.60; found C 64.48, H 5.28, N 17.34. **6a**: IR (KBr): ν = 3232m cm⁻¹, 1671m ν (C=O), 1596m, 1542s, 1515vs ν (N–C=O), 1415m, 1315m, 1258m, 1053m, 945w, 833m, 744m. ¹H NMR (250.13 MHz, 25 °C, DMSO-d₆): δ = 10.84 (s, NH), 8.83 (s, 3H, C₆H₃), 8.62 (d, ³J_{10,11} = 4.3 Hz, H¹¹), 8.56 (d, ³J_{4,5} = 2.0 Hz, H⁵), 8.15–7.94 (m, 6H, H⁸, H⁹, H¹³, H¹⁴), 7.35 (dd, ³J_{9,10} = 7.9 Hz, H¹⁰), 7.12 (d, H⁴), 3.57 (br, 10H, H₂O). ¹³C{¹H} NMR (62.895 MHz, 25 °C, DMSO-d₆): δ = 164.3 (CO), 151.9 (C³), 150.8 (C⁷), 148.9 (C¹¹), 137.3, 137.1, 135.4, 135.2 (C⁹, C¹⁵, 2 × C₆H₃), 130.0 (C¹²), 129.2 (C⁵), 122.9 (C¹⁰), 121.1 (C¹³), 119.7 (C⁸), 118.8 (C¹⁴), 106.3 (C⁴). C₃₄H₃₀N₈O₂ · (H₂O)₃ (995.00): calcd. C 64.14, H 4.85, N 17.60; found C 64.57, H 4.59, N 17.61.

N-(1-Ferrocenylethyliden)(4-(3-(2-pyridyl)pyrazol-1-yl)aniline (**7a1**): 0.50 g (2.12 mmol) of **3a** and 0.48 g (2.12 mmol) of acetyl ferrocene are dissolved in a Schlenk tube in 30 ml of toluene. 0.30 g of neutral and 0.30 g of acidic alumina are added and the orange solution is heated to reflux for 4 h. The alumina is filtered off and the solvent is evaporated in vacuum leaving 0.35 g (37%) of **7a1** as a red-brown solid. IR (KBr): ν = 3207m cm⁻¹, 1669m ν (C=N), 1626vs, 1589m, 1507s, 1456m, 1368m, 1269m, 1231s, 1167m, 1116m, 1053m, 1005m, 855m, 816m, 768s, 681m, 561m. ¹H NMR (250.13 MHz, 25 °C, CDCl₃): δ = 8.55 (d, ³J_{10,11} = 4.0 Hz, H¹¹), 8.03 (d, ³J_{8,9} = 7.9 Hz, H⁸), 7.84 (d, ³J_{4,5} = 1.7 Hz, H⁵), 7.64–7.61 (m, 2H, H⁹, H¹³), 7.09 (dd, ³J_{9,10} = 7.9 Hz, H¹⁰), 7.02 (d, H⁴), 6.76 (d, 2H, ³J_{13,14} = 8.4 Hz, H¹⁴), 4.69, 4.31 (2 × s, 2 × 2H, C₅H₄), 4.01 (s, 5H, C₅H₅), 1.99 (s, 3H, CH₃). ¹³C{¹H} NMR (62.895 MHz, 25 °C, CDCl₃): δ = 168.4 (C=N), 152.8 (C³), 152.0 (C⁷), 150.6 (C¹¹), 149.3 (C¹⁵), 136.5 (C⁹), 135.7 (C¹²), 128.2 (C⁵), 122.5 (C¹⁰), 120.5 (C¹³), 120.1 (C⁸), 102.1 (C¹⁴), 106.1 (C⁴), 83.3 (i-C₅H₄), 70.7,

68.3 (o-, p-C₅H₄), 69.5 (C₅H₅), 18.1 (CH₃). C₂₆H₂₂FeN₄ · (CH₂Cl₂)_{0.33} (474.64): calcd. C 66.64, H 4.81, N 11.80; found C 66.83, H 4.41, N 11.93.

N-(1-Ferrocenylmethylene)(4-(3-(2-pyridyl)pyrazol-1-yl)-aniline (**8a1**), *N,N'*-(1,1'-ferrocenylendimethylidene)bis(4-(3-(2-pyridyl)pyrazol-1-yl)aniline (**8a2**): 1.00 g (4.23 mmol) of **3a** and 0.90 g (4.23 mmol) of ferrocenyl aldehyde (or 0.51 g (2.12 mmol) of ferrocenyl-1,1'-dialdehyde, resp.) are dissolved in methanol and heated to reflux for 2 h. The solvent is removed in vacuum and the red-brown residue is recrystallized from ethyl acetate or chloroform. Yields: **8a1**, 1.28 g (70.1%) of a brown microcrystalline solid; **8a2**, 0.82 g (57%) of a red-brown crystalline solid. **8a1**: IR (KBr): $\nu = 3088\text{m cm}^{-1}$, 1734w, 1622vs $\nu(\text{C}=\text{N})$, 1593s, 1507vs, 1486m, 1458m, 1385m, 1365m, 1308w, 1280m, 1265m, 1215m, 1189w, 1123w, 1104m, 1037m, 996m, 968w, 942w, 861m, 832m, 797m, 764s, 713m, 690w, 622w, 502m, 481m. ¹H NMR (250.13 MHz, 25 °C, CDCl₃): $\delta = 8.58$ (d, ³J_{10,11} = 4.4 Hz, H¹¹), 8.30 (s, CH=N), 8.04 (d, ³J_{8,9} = 7.9 Hz, H⁸), 7.90 (d, ³J_{4,5} = 2.1 Hz, H⁵), 7.75–7.64 (m, 3H, H⁹, H¹³), 7.19–7.13 (m, 3H, H¹⁰, H¹⁴), 7.06 (d, H⁴), 4.74, 4.43 (2 × s, 2 × 2H, C₅H₄), 4.18 (s, 5H, C₅H₅). ¹³C{¹H} NMR (62.895 MHz, 25 °C, CDCl₃): $\delta = 161.6$ (CH=N), 151.9 (C³), 151.1 (C⁷), 149.4 (C¹¹), 148.4 (C¹⁵), 136.5 (C⁹), 135.4 (C¹²), 128.1 (C⁵), 122.7 (C¹⁰), 121.5 (C¹³), 120.3 (C⁸), 120.0 (C¹⁴), 106.4 (C⁴), 80.1 (i-C₅H₄), 71.5, 69.3 (o-, p-C₅H₄), 69.6 (C₅H₅). C₂₅H₂₀FeN₄ (432.30): calcd. C 69.46, H 4.66, N 12.96; found C 68.87, H 4.44, N 12.77. **8a2**: IR (KBr): $\nu = 1620\text{s cm}^{-1}$ $\nu(\text{C}=\text{N})$, 1529m, 1509vs, 1485m, 1457m, 1417m, 1367s, 1313w, 1266m, 1126w, 1046m, 943m, 835m, 751m, 712m, 620w. ¹H NMR (250.13 MHz, 25 °C, CDCl₃): $\delta = 8.64$ (s, H¹¹), 8.30 (s, CH=N), 8.06 (d, ³J_{8,9} = 7.0 Hz, H⁸), 7.85 (s, H⁵), 7.68–7.65 (m, 3H, H⁹, H¹³), 7.16–7.13 (m, 3H, H¹⁰, H¹⁴), 7.01 (s, H⁴), 4.92, 4.54 (2 × s, 2 × 2H, C₅H₄). ¹³C{¹H} NMR (62.895 MHz, 25 °C, CDCl₃): $\delta = 160.1$ (CH=N), 152.8 (C³), 151.7 (C⁷), 150.1 (C¹¹), 149.1 (C¹⁵), 137.4 (C¹²), 136.3 (C⁹), 127.9 (C⁵), 122.4 (C¹⁰), 121.4 (C¹³), 120.1 (C⁸), 119.6 (C¹⁴), 106.3 (C⁴), 81.5 (i-C₅H₄), 72.0, 70.0 (o-, p-C₅H₄). C₄₀H₃₀FeN₈ · (MeOH) (710.62): calcd. C 69.30, H 4.82, N 15.77; found C 69.52, H 4.45, N 15.65.

Single crystal X-ray structure determination of compounds **2a**, **4a**, and **8a2**

2a: Crystal data and details of the structure determination are presented in Table 1. Suitable single crystals for the X-ray diffraction study were grown from diethylether. A clear dark red plate was stored under perfluorinated ether, transferred in a Lindemann capillary, fixed, and sealed. Preliminary examination and data collection were carried out on an imaging plate device (NONIUS, DIP2020) equipped with a NONIUS cooling system at the window of a sealed tube (NON-

IUS, FR590) and graphite monochromated Mo-K α radiation ($\lambda = 0.71073 \text{ \AA}$). The unit cell parameters were obtained by full-matrix least-squares refinement of 2913 reflections. Data collection were performed at 143 K within a Θ -range of $3.24^\circ < \Theta < 25.35^\circ$. One data set was measured in rotation scan modus with $\Delta\phi = 2.0^\circ$. A total number of 20272 intensities were integrated. Raw data were corrected for Lorentz, polarization, and, arising from the scaling procedure, for latent decay and absorption effects. After merging ($R_{\text{int}} = 0.036$) a sum of 2729 (all data) and 2715 [$I > 2\sigma(I)$], respectively, remained and all data were used. The structure was solved by a combination of direct methods and difference Fourier syntheses. All non-hydrogen atoms were refined with anisotropic displacement parameters. All hydrogen atom positions were found in the difference map calculated from the model containing all non-hydrogen atoms. The hydrogen positions were refined with individual isotropic displacement parameters. Full-matrix least-squares refinements with 302 parameters were carried out by minimising $\Sigma w(F_o^2 - F_c^2)^2$ with SHELXL-97 weighting scheme and stopped at shift/err < 0.002. The final residual electron density maps showed no remarkable features. Neutral atom scattering factors for all atoms and anomalous dispersion corrections for the non-hydrogen atoms were taken from *International Tables for Crystallography*. All calculations were performed on an Intel Pentium II PC, with the STRUX-V system, including the programs PLATON, SIR92, and SHELXL-97 [14].

4a: Crystal data and details of the structure determination are presented in Table 1. Suitable single crystals for the X-ray diffraction study were grown from ethyl acetate. A clear pale yellow fragment was stored under perfluorinated ether, transferred in a Lindemann capillary, fixed and sealed. Preliminary examination and data collection were carried out on an area detecting system (NONIUS, MACH3, κ -CCD) at the window of a rotating anode (NONIUS, FR951) and graphite monochromated Mo-K α radiation ($\lambda = 0.71073 \text{ \AA}$). The unit cell parameters were obtained by full-matrix least-squares refinement of 4115 reflections. Data collection were performed at 123 K within a Θ -range of $1.71^\circ < \Theta < 25.35^\circ$. Nine data sets were measured in rotation scan modus with $\Delta\phi/\Delta\Omega = 1.0^\circ$. A total number of 46656 intensities were integrated. Raw data were corrected for Lorentz, polarization, and, arising from the scaling procedure, for latent decay and absorption effects. After merging ($R_{\text{int}} = 0.039$) a sum of 3845 (all data) and 3481 [$I > 2\sigma(I)$], respectively, remained and all data were used. The structure was solved by a combination of direct methods and difference Fourier syntheses. All non-hydrogen atoms were refined with anisotropic displacement parameters. All hydrogen atom positions were found in the difference map calculated from the model containing all non-hydrogen atoms. The hydrogen positions were refined with individual isotropic displacement parameters. Full-matrix least-squares refinements with 382 param-

	2a	4a	8a2
Empirical formula	C ₁₈ H ₁₀ MoN ₄ O ₆	C ₂₄ H ₃₀ N ₄ O	C ₄₀ H ₃₀ FeN ₈
Formula mass	474.24	390.52	678.57
Crystal system	monoclinic	monoclinic	monoclinic
Space group	<i>P</i> 2 ₁ / <i>c</i> (no. 14) [15]	<i>C</i> 2/ <i>c</i> (no. 15) [15]	<i>P</i> 2 ₁ (no. 4) [15]
<i>a</i> [Å]	15.9797(2)	27.3934(2)	8.1729(1)
<i>b</i> [Å]	9.6750(1)	8.9332(1)	10.2974(1)
<i>c</i> [Å]	12.0986(1)	19.7402(2)	18.9024(2)
β [°]	105.5560(7)	119.4828(6)	102.1477(4)
<i>V</i> [Å ³]	1801.97(3)	4205.09(7)	1555.20(3)
<i>Z</i>	4	8	2
$\rho_{\text{calcd.}}$ [g cm ⁻³]	1.748	1.234	1.449
μ [mm ⁻¹]	0.774	0.077	0.531
<i>T</i> [K]	143	123	123
<i>F</i> (000)	944	1680	704
Crystal size [mm]	0.51 × 0.51 × 0.18	0.46 × 0.30 × 0.10	0.51 × 0.51 × 0.10
Θ -Range [°]	3.24/25.35	1.71/25.35	2.20/25.33
Index ranges	<i>h</i> : ±14/ <i>k</i> : ±11/ <i>l</i> : ±14	<i>h</i> : ±32/ <i>k</i> : ±10/ <i>l</i> : ±23	<i>h</i> : ±9/ <i>k</i> : ±12/ <i>l</i> : ±22
Reflections collected	20272	46656	32859
Independent reflections	2715/2729/0.036	3481/3845/0.039	5431/5688/0.049
[<i>I</i> _o > 2 σ (<i>I</i> _o)/all data/ <i>R</i> _{int}]			
Data/restraints/parameters	2729/0/302	3845/0/382	5688/1/442
<i>R</i> 1 [<i>I</i> _o > 2 σ (<i>I</i> _o)/all data]	0.0250/0.0250	0.0381/0.0433	0.0322/0.0348
<i>wR</i> 2 [<i>I</i> _o > 2 σ (<i>I</i> _o)/all data]	0.0696/0.0697	0.0917/0.0971	0.0743/0.0756
<i>GOF</i>	1.054	1.074	1.051
Weights <i>a/b</i>	0.0468/1.3233	0.0482/3.1058	0.0295/0.8296
$\Delta\rho_{\text{max/min}}$ [e·Å ⁻³]	0.37/−0.62	0.18/−0.22	0.24/−0.30

Table 1. Summary of the crystallographic data and details of data collection and refinement for compounds **2a**, **4a**, and **8a2**.

eters were carried out by minimising $\Sigma w(F_o^2 - F_c^2)^2$ with SHELXL-97 weighting scheme and stopped at shift/err < 0.001. The final residual electron density maps showed no remarkable features. Neutral atom scattering factors for all atoms and anomalous dispersion corrections for the non-hydrogen atoms were taken from *International Tables for Crystallography*. All calculations were performed on an Intel Pentium II PC, with the STRUX-V system, including the programs PLATON, SIR92, and SHELXL-97 [14].

8a2: Crystal data and details of the structure determination are presented in Table 1. Suitable single crystals for the X-ray diffraction study were grown from chloroform. A clear red plate was stored under perfluorinated ether, transferred in a Lindemann capillary, fixed and sealed. Preliminary examination and data collection were carried out on an area detecting system (NONIUS, MACH3, κ -CCD) at the window of a rotating anode (NONIUS, FR951) and graphite monochromated Mo-K α radiation ($\lambda = 0.71073$ Å). The unit cell parameters were obtained by full-matrix least-squares refinement of 3020 reflections. Data collection was performed at 123 K within a Θ -range of $2.20^\circ < \Theta < 25.33^\circ$. Nine data sets were measured in rotation scan modulus with $\Delta\phi/\Delta\Omega = 1.0^\circ$. A total number of 32859 intensities were integrated. Raw data were corrected for Lorentz, polarization, and, arising from the scaling procedure, for latent decay and absorption effects. After merging (*R*_{int} = 0.049) a sum of 5688 (all data) and 5431 [*I* > 2 σ (*I*)], respectively, remained and all data were used. The structure was solved by a combination

of direct methods and difference Fourier syntheses. All non-hydrogen atoms were refined with anisotropic displacement parameters. All hydrogen atom positions were calculated in ideal positions (riding model). Full-matrix least-squares refinements with 442 parameters were carried out by minimizing $\Sigma w(F_o^2 - F_c^2)^2$ with SHELXL-97 weighting scheme and stopped at shift/err < 0.001. The final residual electron density maps showed no remarkable features. The correct enantiomere is proved by Flack's parameter $\epsilon = 0.01(1)$. Neutral atom scattering factors for all atoms and anomalous dispersion corrections for the non-hydrogen atoms were taken from *International Tables for Crystallography*. All calculations were performed on an Intel Pentium II PC, with the STRUX-V system, including the programs PLATON, SIR92, and SHELXL-97 [14].

Crystallographic data (excluding structure factors) for the structures reported in this paper have been deposited with the Cambridge Crystallographic Data Centre as supplementary publication nos. CCDC 246780 (**2a**), CCDC 246360 (**4a**), and CCDC 246781 (**8a2**). Copies of the data can be obtained free of charge on application to CCDC, 12 Union Road, Cambridge CB2 1EZ, UK (fax: (+44)1223-336-033; e-mail: deposit@ccdc.cam.ac.uk).

Acknowledgement

The authors thank the Deutsche Forschungsgemeinschaft for generous support of this work.

- [1] H. Brunner, T. Scheck, *Chem. Ber.* **125**, 701 (1992).
- [2] a) R. Fusco, in R. H. Wiley (ed): *The Chemistry of Heterocyclic Compounds: Pyrazoles, Pyrazolines, Pyrazolidines, Indazoles and Condensed Rings*, Vol. 22, p. 1–174, J. Wiley & Sons, New York (1967); b) W. R. Thiel, J. Eppinger, *Chemistry Eur. J.* **3**, 696 (1997); c) M. A. Khan, A. A. A. Pinto, *J. Heterocycl. Chem.* **18**, 9 (1981).
- [3] a) W. R. Thiel, M. Angstl, T. Priermeier, *Chem. Ber.* **127**, 2373 (1994); b) W. R. Thiel, T. Priermeier, *Angew. Chem.* **107**, 1870 (1995); *Angew. Chemie Int. Ed. Engl.* **34**, 1737 (1995); c) H. Glas, M. Spiegler, W. R. Thiel, *Eur. J. Inorg. Chem.* **1**, 275 (1998); d) H. Glas, E. Herdtweck, G. R. J. Artus, W. R. Thiel, *Inorg. Chem.* **37**, 3644 (1998); e) M. Barz, H. Glas, W. R. Thiel, *Synthesis* 1269 (1998); f) M. Jia, W. R. Thiel, *Chem. Commun.* 2392 (2002); g) M. Jia, A. Seifert, M. Berger, H. Giegengack, S. Schulze, W. R. Thiel, *Chem. Mat.* **16**, 877 (2004); h) M. J. Hinner, M. Grosche, E. Herdtweck, W. R. Thiel, *Z. Anorg. Allg. Chem.* **629**, 2251 (2003).
- [4] a) R. E. Sammelson, J. E. Casida, *J. Org. Chem.* **68**, 8075 (2003); b) N. W. Gilman, B. C. Holland, G. R. Walsh, R. I. Fryer, *J. Heterocycl. Chem.* **14**, 1157 (1977); c) F. Pietra, F. Del Cima, *J. Chem. Soc., Perkin Trans.* 1420 (1972); d) T. Kitazaki, T. Ichikawa, A. Tasaka, H. Hosono, Y. Matsushita, R. Hayashi, K. Okonogi, K. Itoh, *Chem. Pharm. Bull.* **48**, 1935 (2000); e) X. Wang, J. Tan, L. Zhang, *Org. Lett.* **2**, 3107 (2000); f) X. Wang, J. Tan, K. Grozinger, R. Betageri, T. Kirrane, J. R. Proudfoot, *Tetrahedron Lett.* **41**, 5321 (2000); g) M. L. Cerrada, J. Elguero, J. de la Fuente, C. Pardo, M. Ramos, *Synth. Commun.* **23**, 1947 (1993); h) J. Rosevear, J. F. K. Wilshire, *Austr. J. Chem.* **44**, 1097 (1991); i) N. W. Gilman, R. I. Fryer, *J. Heterocycl. Chem.* **14**, 1171 (1977).
- [5] a) Y. Luo, P. G. Potvin, *J. Org. Chem.* **59**, 1761 (1994); b) P. van der Falk, P. G. Potvin, *J. Org. Chem.* **59**, 1766 (1994).
- [6] B. L. Shaw, S. D. Perera, D. J. Shenton, M. Thornton-Pett, *Inorg. Chim. Acta* **270**, 312 (1998).
- [7] A. L. Spek, PLATON, A Multipurpose Crystallographic Tool, Utrecht University, Utrecht, The Netherlands (2000).
- [8] A. L. Spek, PLUTON, A program for plotting molecular and crystal structures, University of Utrecht, The Netherlands (1995).
- [9] a) K. Heinze, *J. Chem. Soc., Dalton Trans.* 540 (2002); b) I. Veroni, A. Rontoyianni, C. A. Mitsopoulou, *J. Chem. Soc., Dalton Trans.* 255 (2003); c) P. N. W. Baxter, J. A. Connor, J. D. Wallis, D. C. Povey, *J. Organomet. Chem.* **426**, 187 (1992); d) P. N. W. Baxter, J. A. Connor, J. D. Wallis, D. C. Povey, A. K. Powell, *Polyhedron* **11**, 1771 (1992); e) X.-J. Xie, X.-L. Jin, K.-L. Tang, *Acta Crystallogr., Sect. C* **57**, 696 (2001); f) W. A. Herrmann, W. R. Thiel, J. G. Kuchler, J. Behm, E. Herdtweck, *Chem. Ber.* **123**, 1963 (1990).
- [10] W. R. Thiel, T. Priermeier, D. A. Fiedler, A. M. Bond, M. R. Mattner, *J. Organomet. Chem.* **514**, 137 (1996).
- [11] T. Steiner, *Angew. Chem.* **114**, 50 (2002); *Angew. Chem. Int. Ed.* **41**, 48 (2002).
- [12] a) T. Moriuchi, K. Yoshida, T. Hirao, *J. Organomet. Chem.* **637**, 75 (2001); b) H. Butcher, T. A. Hamor, I. L. Martin, *Acta Crystallogr., Sect. C* **39**, 1469 (1983); c) H. Miyaji, M. Dudic, J. H. R. Tucker, I. Prokes, M. E. Light, M. B. Hursthouse, I. Stibor, P. Lhotak, *Tetrahedron Lett.* **43**, 873 (2002); d) J. P. Collman, J. I. Brauman, J. P. Fitzgerald, P. D. Hampton, Y. Naruta, J. W. Sparapany, J. A. Ibers, *J. Am. Chem. Soc.* **110**, 3477 (1988); e) C. C. Forbes, A. M. Beatty, B. D. Smith, *Organic Letters* **3**, 3595 (2001); f) N. Boubals, M. G. B. Drew, C. Hill, M. J. Hudson, P. B. Iveson, C. Madic, M. L. Russell, T. G. A. Youngs, *J. Chem. Soc., Dalton Trans.* 55 (2002); g) I. L. Karle, D. Ranganathan, V. Haridas, *J. Am. Chem. Soc.* **119**, 2777 (1997); h) R. Sonnenburg, I. Neda, A. Fischer, P. G. Jones, R. Schmutzler *Z. Naturforsch.* **49b**, 788 (1994).
- [13] K. Kunz, G. Erker, G. Kehr, R. Fröhlich, *Organometallics* **20**, 392 (2001).
- [14] a) Data Collection Software for NONIUS κ -CCD devices, Delft, The Netherlands, (1997); b) Z. Otwinowski, W. Minor, *Methods in Enzymology* **276**, 307 (1997); c) G. Artus, W. Scherer, T. Priermeier, E. Herdtweck, STRUX-V: A Program System to Handle X-Ray Data, TU München, Garching, Germany (1997); d) A. Altomare, G. Casciaro, C. Giacovazzo, A. Guagliardi, M. C. Burla, G. Polidori, M. Camalli, SIR92, *J. Appl. Crystallogr.* **27**, 435 (1994); e) G. M. Sheldrick, SHELXL-97, University of Göttingen, Göttingen, Germany (1998).
- [15] International Tables for Crystallography, Vol. A, Kluwer Academic Publishers, Dordrecht (1992).